Available online at www.medicinescience.org

ORIGINAL ARTICLE

Medicine Science International Medical Journal

Medicine Science 2026;15(3):1226-33

Assessment of retinal neurodegeneration in prediabetes, type 1, and type 2 diabetes using swept-source optical coherence tomography

Cigdem Deniz Genc[1], Esra Isik Tokur[2], Gokhan Ozgur[3], Emre Aydin[1], Saban Kilic[1], Muhammed Mustafa Kurt[1]

[1]Samsun University Faculty of Medicine, Department of Ophthalmology, Samsun, Türkiye
[2]Osmangazi Family Health Center, Department of Family Medicine, Samsun, Türkiye
[3]Medicana International Samsun Hospital, Department of Ophthalmology, Samsun, Türkiye

Received 24 April 2026; Accepted 09 July 2026
Available online 15 August 2026 with doi: 10.5455/medscience.2026.04.088

Abstract

The objective of this research was to assess initial neurodegenerative changes in individuals diagnosed with prediabetes, type 1, and type 2 diabetes via optical coherence tomography (OCT). By analyzing the macula, retinal nerve fiber layer (RNFL), ganglion cell–inner plexiform layer (GCL+) and ganglion cell complex (GCL++), we sought to determine structural variations compared to a healthy cohort. This retrospective investigation evaluated the right eyes of 147 subjects aged 18 years and above. The cohort was categorized into four distinct groups: healthy controls, prediabetes, type 1 diabetes mellitus (DM), and type 2 DM. Macular, RNFL, GCL+, and GCL++ thicknesses were quantified utilizing high-resolution scans from a swept-source OCT device. The type 1 DM cohort exhibited significantly greater GCL++ and superior parafoveal (PF) macular thicknesses relative to the control and prediabetic subjects. Conversely, RNFL and GCL+ measurements did not differ significantly among the groups. While GCL++ dimensions showed no notable correlation with Hemoglobin A1c (HbA1c) levels across any category, GCL+ thickness demonstrated a negative correlation in the superior quadrant for healthy controls and a positive correlation in the superotemporal quadrant for the type 2 DM group. These findings imply that traditional atrophic retinal neurodegeneration might not be initiated in these early stages, or that initial metabolic stress merely presents as localized reactive swelling. It appears that early diabetic neural impairment is a reaction to accumulated metabolic stress—rather than sudden glycemic shifts—progressing in a layer-specific manner before any clinical microangiopathy becomes evident.

Keywords: Diabetes mellitus, neurodegeneration, optical coherence tomography, prediabetes, retinal ganglion cells

Introduction

Diabetes mellitus (DM) is a chronic metabolic disorder of increasing global prevalence and encompasses a group of metabolic disturbances characterized by elevated blood glucose levels [1]. In the literature, the ocular complications of diabetes are considered to begin with clinically detectable microvascular damage [2]. However, clinical and experimental studies conducted in recent years have fundamentally challenged this belief, demonstrating that neurodegeneration at the cellular level begins years before vascular changes occur [3,4]. This early toxic effect of impaired glucose metabolism on neural tissues has necessitated the investigation of diabetes-related neurodegeneration as a distinct pathophysiological process [2]. Chronic hyperglycemia has been reported to exert significant effects not only on retinal layers but also on intraocular pressure (IOP) dynamics, and IOP control in diabetic populations has been identified as a critical parameter for neuroprotection [5,6].

Today, high-resolution Optical Coherence Tomography (OCT) has become the most reliable imaging method for detecting these early subclinical neurodegenerative changes in vivo [7,8]. The literature reports that structural changes in the retinal

CITATION
Deniz Genc C, Isik Tokur E, Ozgur G, et al. Assessment of retinal neurodegeneration in prediabetes, type 1, and type 2 diabetes using swept-source optical coherence tomography. Med Science. 2026;15(3):1226-33.

Corresponding Author: Cigdem Deniz Genc, Samsun University Faculty of Medicine, Department of Ophthalmology, Samsun, Türkiye
Email: cigdem.deniz@samsun.edu.tr

DOI: 10.5455/medscience.2026.04.088

nerve fiber layer (RNFL) and, in particular, in the ganglion cell complex (GCL++) thickness in diabetic patients serve as sensitive indicators of early neuronal dysfunction [9]. At this point, the clinical similarity between the neural damage caused by diabetes and that of glaucoma is striking. Glaucoma is an irreversible and progressive optic neuropathy that can lead to severe visual field loss and blindness [10]. The structural retinal damage that occurs in the development of glaucomatous optic neuropathy (GON), much like in diabetes, is characterized by the progressive loss of retinal ganglion cells (RGCs) and atrophy of the nerve fiber layer [11]. Traditionally used as key structural parameters in the differential diagnosis of GON, these measures have also been shown, in light of current evidence, to have a similar clinical importance in detecting early neural damage in diabetes [7]. However, comprehensive studies comparing structural retinal changes in the prediabetic stage when glucose tolerance first becomes impaired with the neurodegenerative profiles of type 1 and type 2 diabetes within the same cohort using detailed complex parameters such as GCL++ remain limited in the literature [12,13].

The aim of this study was to evaluate macular, RNFL, and GCL++ parameters using OCT in patients with prediabetes, type 1 diabetes, and type 2 diabetes, thereby assessing early neurodegeneration and identifying differences compared with the normal population.

Material and Methods

Participants

This research evaluated the right eyes of 147 subjects aged 18 years and above, categorized into a healthy control cohort, prediabetic individuals, and patients diagnosed with either Type 1 or Type 2 diabetes who exhibited no clinical signs of retinopathy. This study was conducted at the Department of Ophthalmology, Samsun Training and Research Hospital, utilizing a retrospective review of comprehensive electronic medical records and imaging data collected between January 1, 2020 and June 1, 2023. The data extraction and formal review process commenced in June 2023, following the ethical approval granted on June 7, 2023. The optimal number of subjects was determined using the G×Power 3.1 program. Sample size estimation was conducted for a four-group one-way analysis of variance (ANOVA), aiming for an 80% statistical power and an alpha error margin of 0.05 based on a large anticipated effect size (Cohen's f = 0.40). Based on these parameters, the minimum required total sample size was calculated as 76 participants (19 per group). With a total of 147 enrolled participants, our study substantially exceeded this minimum requirement, ensuring adequate statistical power to detect meaningful structural differences. As this study was a retrospective chart review and anonymized data obtained during routine outpatient follow-up were used, an informed consent waiver was granted by the ethics committee. All research procedures were conducted as per the principles of the Declaration of Helsinki.

Study Design

This retrospective observational study was approved by the Scientific Research and Publication Ethics Committee of Samsun University (Approval No: 2023 11/4, Date: 07.06.2023) and was conducted as per the Declaration of Helsinki. The inclusion criteria were being over the age of 18 years, having prediabetes (impaired fasting glucose 100–125 mg/dL, impaired glucose tolerance 140–199 mg/dL, or Hemoglobin A1c (HbA1c) levels between 5.7% and 6.4%), diagnosis of type 1 or type 2 diabetes mellitus or belonging to the control group, and absence of any other ocular pathology that could affect OCT imaging. Exclusion criteria encompassed participants younger than 18 years, a documented history of eye surgeries, prior intracranial diseases or head trauma, spherical equivalent (SE) refractive errors exceeding ± 3.0 diopters, astigmatism exceeding ± 1.0 diopters, axial lengths > 26 mm, concurrent ocular conditions like uveitis or glaucoma, and any degree of amblyopia.

Procedures

Comprehensive ophthalmological assessment data of all participants, recorded in the hospital automation system, were retrospectively reviewed. Visual acuity (VA, logMAR), refractive status, and anterior segment examination findings obtained via slit-lamp biomicroscopy were recorded from the patient records. Furthermore, intraocular pressure (IOP) values measured via Goldmann applanation tonometry (Haag-Streit, Koeniz, Switzerland) and central corneal thickness (CCT) measurements obtained using a Topcon CT-1P device (Topcon, Tokyo, Japan) were extracted from the comprehensive clinical database. Patients' blood glucose regulation profiles (impaired fasting glucose, impaired glucose tolerance, and HbA1c levels) were obtained from the system to evaluate the systemic parameters of the study. Given that HbA1c reflects the average glycemic control over the preceding 8–12 weeks, we included patients whose corresponding blood test results were obtained from the comprehensive electronic health record system within a maximum interval of three months relative to the swept-source optical coherence tomography (SS-OCT) imaging date. For the structural assessment of the retinal layers, high-resolution images obtained using a swept-source OCT device during routine outpatient examinations were utilized. Macular thickness, RNFL, ganglion cell layer (GCL+) and GCL++ thicknesses were analyzed using these images. To ensure measurement reliability and data standardization, OCT images with low signal strength or containing artifacts were excluded from the study, and the final analysis and recording of all OCT measurements were performed by a single experienced ophthalmologist.

OCT Measurement Protocol

Retinal layer quantifications were acquired via a Topcon DRI Triton SS-OCT scanner (Topcon, Tokyo, Japan). This instrument operates at a 1050-nm wavelength with a scanning velocity of 100,000 A-scans per second, offering an 8-μm

DOI: 10.5455/medscience.2026.04.088

axial and 20-µm transverse resolution. This technology produces high-quality images that enable detailed analysis of the deep layers of the retina [14]. The 3D Wide protocol, which includes a wide scanning range (12 × 9 mm) focusing on both the macular and peripapillary areas, was used in the scans. Macular thickness was assessed in the foveal, parafoveal (PF), and pericentral (PCR) regions. RNFL thickness was measured between the inner limiting membrane (ILM) and the GCL boundaries. GCL was defined between two distinct boundaries: while GCL+ thickness was measured between the RNFL and the inner nuclear layer (INL), GCL++ thickness was measured between the ILM and the INL. All GCL+ and GCL++ thickness measurements were assessed in six different quadrants of the macula (superior, superonasal, superotemporal, inferior, inferonasal, and inferotemporal). The DRI Triton SS-OCT device features an image quality scale for determining signal strength. The signal strength index (SSI) ranges from 0 (poor quality) to 100 (excellent quality). In this retrospective study, images with an SSI score below 55 or containing significant artifacts were excluded from the analysis to ensure measurement reliability. During the initial visual screening, scans exhibiting obvious automated segmentation failures or severe algorithmic errors were entirely excluded from the dataset (Figure 1).

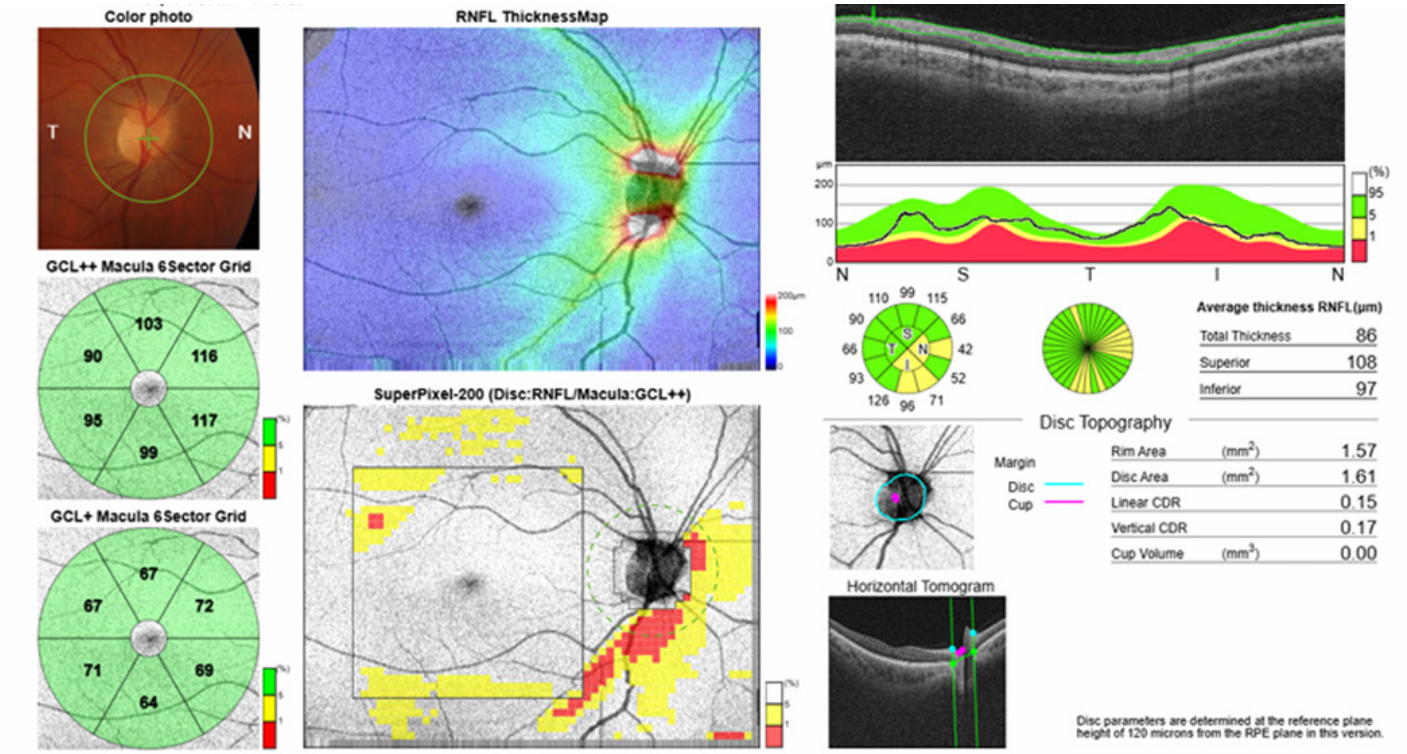

Figure 1. 1 SS-OCT of a patient. GCL++ and GCL+ thickness of SS-OCT; SS-OCT: swept source optical coherence tomography, GCC: ganglion cell complex, GCIPL: ganglion cell-inner plexiform layer, GCL: ganglion cell layer, RNFL: retina nerve fiber layer; GCL+, GCIPL; GCL++, GCIPL + RNFL

Statistical Analysis

The SPSS program (SPSS for Windows, version 23.0, SPSS Inc., Chicago, Illinois, USA) was used for statistical analyses. The data were presented as mean and standard deviation. The Shapiro-Wilk test was applied for normality, the Levene test for homogeneity, and it was determined that the data showed a normal distribution. One-way analysis of variance (ANOVA) was used to compare ocular structural parameters among the study groups (control, prediabetes, type 1 diabetes mellitus, and type 2 diabetes mellitus). Tukey's Honestly Significant Difference (HSD) post hoc test was performed for pairwise comparisons of groups in parameters where statistically significant differences were detected. Pearson correlation analysis was used to assess the correlation between HbA1c levels and OCT parameters. Partial eta-squared values were calculated to determine the effect sizes (ES). Statistical results were evaluated at a 95% confidence interval and a significance level of $p < 0.05$.

Results

The comparison of the demographic and basic clinical characteristics of the groups is presented in Table 1. Significant differences were observed in the body mass index (BMI) (0.014), age ($p < 0.001$), and HbA1c ($p < 0.001$) parameters ($p < 0.005$).

DOI: 10.5455/medscience.2026.04.088

Table 1. Demographic and clinical characteristics of the study population

Variables		Control (n = 29)	Prediabetes (n = 31)	Type I (n = 31)	Type II (n = 56)	*p*
		Mean ± SD	Mean ± SD	Mean ± SD	Mean ± SD	
BMI (kg/m²)		23.83 ± 3.52^{ab}	23.46 ± 1.68^{b}	24.33 ± 1.37^{ab}	24.92 ± 1.67^{a}	0.014*
Age (year)		52.66 ± 8.06^{b}	51.13 ± 8.64^{b}	39.84 ± 6.97^{b}	58.24 ± 9.87^{a}	< 0.001***
VA (logMAR)		1.00 ± 0.00	0.99 ± 0.04	0.98 ± 0.06	0.99 ± 0.02	0.373
IOP (mmHg)		16.14 ± 2.74	15.87 ± 2.81	15.23 ± 2.33	15.52 ± 2.55	0.532
CCT (µm)		557.38 ± 18.58	546.16 ± 24.07	554.23 ± 18.17	551.27 ± 19.67	0.169
HbA1c (%)		5.30 ± 0.29^{b}	5.94 ± 0.29^{b}	8.01 ± 1.80^{a}	7.87 ± 1.21^{a}	< 0.001***
Gender (n/%)	**Female**	17/58.62	21/67.74	16/51.61	35/62.50	
	Male	12/41.38	10/32.26	15/48.39	21/37.50	

*p < 0.05; **p < 0.01; BMI: body mass index, µm: micrometer, SD: standard deviation, VA: visual acuity, IOP: intraocular pressure, CCT: central corneal thickness, HbA1c: hemoglobin A1c, F: female, M: male; Different superscript letters (a, b, c) in the same row indicate a statistically significant difference between the group (p < 0.05)

Table 2 presents a comparison of GCL++ parameters across groups. When the results were examined, there was statistical significance (p < 0.05) between the superior parameter of Type I and the control group; the superonasal parameter of Type I and both the control and Type II groups; the superotemporal parameter of Type I and both the control and pre-diabetes groups; the inferior parameter of Type I and the control group; the inferonasal parameter of Type I and both the control and Type II groups; and the inferotemporal parameter of Type I and the control group.

Table 3 presents a comparison of GCL+ parameters across groups. Upon analysis of the results, none of the parameters demonstrated statistical significance (p > 0.05).

Table 2. Intergroup comparison of right-eye GCL++ parameters measured by OCT

Variables (µm)	Control	Prediabetes	Type I	Type II	F	p	η^2	95% CI for η^2_p	
	Mean ± SD	Mean ± SD	Mean ± SD	Mean ± SD				Lower	Upper
Superior	106.7 ± 6.641^{b}	108.9 ± 6.577^{ab}	113.7 ± 9.349^{a}	110.0 ± 8.616^{ab}	4.081	**0.008****	0.079	0.006	0.162
Superonasal	116.5 ± 6.663^{b}	119.2 ± 7.0.87^{ab}	125.4 ± 13.060^{a}	119.4 ± 10.012^{b}	4.594	**0.004****	0.088	0.011	0.174
Superotemporal	94.38 ± 5.596^{b}	95.26 ± 4.464^{b}	100.48 ± 9.423^{a}	98.21 ± 8.727^{ab}	4.222	**0.007****	0.081	0.007	0.166
Inferior	106.5 ± 5.200^{b}	108.3 ± 6.331^{ab}	112.3 ± 9.307^{a}	107.7 ± 9.323^{ab}	3.062	**0.030***	0.060	0.000	0.136
Inferonasal	116.7 ± 6.178^{b}	120.0 ± 7.679^{ab}	124.6 ± 11.147^{a}	119.3 ± 8.869^{b}	4.379	**0.006****	0.084	0.009	0.169
Inferotemporal	97.28 ± 5.182^{b}	98.42 ± 5.965^{ab}	103.39 ± 9.365^{a}	101.71 ± 9.269^{ab}	4.034	**0.009****	0.078	0.006	0.161

*p < 0.05; **p < 0.01; OCT: optical coherence tomography, F: one-way ANOVA test statistic, SD: standard deviation, µm: micrometer, GCL++: ganglion cell complex, CI: confidence interval; partial eta-squared effect value; Different superscript letters (a, b, c) in the same row indicate a statistically significant difference between the group (p < 0.05)

Table 3. Intergroup comparison of right-eye GCL+ parameters measured by OCT

Variables (µm)	Control	Prediabetes	Type I	Type II	F	p	η^2	95% CI for η^2_p	
	Mean ± SD	Mean ± SD	Mean ± SD	Mean ± SD				Lower	Upper
Superior	70.31 ± 4.098	71.26 ± 4.359	73.19 ± 5.552	70.96 ± 6.114	1.722	0.165	0.035	0.000	0.097
Superonasal	75.07 ± 5.028	76.45 ± 4.381	78.23 ± 6.515	75.14 ± 6.662	2.153	0.096	0.043	0.000	0.110
Superotemporal	70.38 ± 4.039	70.97 ± 4.029	73.55 ± 5.881	72.75 ± 5.822	2.655	0.051	0.053	0.000	0.125
Inferior	68.86 ± 4.573	69.71 ± 3.968	69.97 ± 5.128	68.77 ± 6.296	0.472	0.702	0.010	0.000	0.044
Inferonasal	73.76 ± 4.041	75.65 ± 4.184	76.71 ± 6.533	75.04 ± 6.912	1.244	0.262	0.027	0.000	0.083
Inferotemporal	71.69 ± 4.294	71.94 ± 5.118	74.13 ± 5.778	74.29 ± 6.463	2.157	0.096	0.043	0.000	0.111

*p < 0.05; **p < 0.01; OCT: optical coherence tomography, F: one-way ANOVA test statistics, µm: micrometer, SD: standard deviation, GCL+:ganglion cell layer–inner plexiform layer, CI: confidence interval; partial eta-squared effect value

DOI: 10.5455/medscience.2026.04.088

Table 4 presents the intergroup comparison of macular thickness parameters measured by OCT. Upon analysis of the results, a statistically significant difference was observed in the PF superior parameter between the Type I control group and prediabetes groups ($p < 0.05$). There were no significant differences in the other parameters ($p > 0.05$).

Table 5 presents the intergroup comparison of RNFL parameters measured by OCT. Upon analysis of the results, none of the parameters demonstrated statistical significance ($p > 0.05$)

Table 4. Intergroup comparison of macular thickness parameters measured by OCT

Variables (µm)	Control	Prediabetes	Type I	Type II	F	p	η^2	95% CI for η^2_p	
	Mean ± SD	Mean ± SD	Mean ± SD	Mean ± SD				Lower	Upper
Fovea	257.1 ± 19.90	246.8 ± 23.75	243.1 ± 25.88	248.9 ± 25.66	1.777	0.154	0.036	0.000	0.098
PCR Superior	304.9 ± 12.02	314.3 ± 12.93	310.4 ± 20.20	307.0 ± 14.50	2.336	0.076	0.047	0.000	0.116
PCR Nasal	305.3 ± 14.26	310.8 ± 17.82	309.7 ± 21.87	303.8 ± 19.67	1.259	0.291	0.026	0.000	0.080
PCR Inferior	300.0 ± 17.65	309.1 ± 15.10	308.5 ± 19.98	302.8 ± 17.38	2.019	0.114	0.041	0.000	0.106
PCR Temporal	295.4 ± 10.53	300.1 ± 15.22	297.9 ± 18.68	296.8 ± 13.79	0.572	0.634	0.012	0.000	0.049
PF Superior	265.1 ± 12.66[b]	274.8 ± 10.30[b]	277.2 ± 14.39[a]	272.0 ± 15.01[ab]	4.449	**0.005****	0.085	0.000	0.171
PF Nasal	288.8 ± 14.14	292.8 ± 10.91	292.5 ± 15.40	286.0 ± 14.43	2.241	0.086	0.045	0.000	0.113
PF Inferior	269.77 ± 11.56	268.45 ± 13.18	264.84 ± 16.13	269.77 ± 11.56	1.028	0.382	0.021	0.000	0.071
PF Temporal	256.6 ± 10.39	260.4 ± 10.24	262.9 ± 18.55	262.0 ± 16.48	1.140	0.335	0.023	0.000	0.075

*p < 0.05; **p < 0.01; OCT: optical coherence tomography, F: one-way ANOVA test statistics, µm: micrometer, SD: standard deviation, CI: confidence interval, partial eta-squared effect value; Different superscript letters (a, b, c) in the same row indicate a statistically significant difference between the group ($p < 0.05$)

Table 5. Intergroup comparison of RNFL parameters measured by OCT

Variables (µm)	Control	Prediabetes	Type I	Type II	F	p	η^2	95% CI for η^2_p	
	Mean ± SD	Mean ± SD	Mean ± SD	Mean ± SD				Lower	Upper
RNFL Total	106.9 ± 7.79	107.9 ± 7.62	110.7 ± 10.16	105.5 ± 12.71	1.702	0.169	0.034	0.000	0.096
Superior	126.2 ± 12.37	127.8 ± 13.60	131.2 ± 14.07	126.3 ± 18.89	0.760	0.518	0.016	0.000	0.059
Inferior	133.1 ± 11.37	139.5 ± 14.34	142.1 ± 19.07	136.9 ± 17.02	1.768	0.156	0.036	0.000	0.098

*p < 0.05; OCT: optical coherence tomography, RNFL: retinal nerve fiber layer, F: one-way ANOVA test statistic, µm: micrometer, SD: standard deviation, CI: confidence interval; partial eta-squared effect value

Table 6 presents the correlation analysis between HbA1c and right-eye GCL++ parameters across all groups. Upon examination of the results, no significant correlation was observed for any of the parameters ($p > 0.05$).

Table 7 presents the correlation analysis between HbA1c and right-eye GCL+ parameters across all groups. Upon analysis of the results, a statistically significant negative correlation was observed in the control group for the superior parameter ($r = -0.444$, $p = 0.016$) ($p < 0.05$). In the Type II group, there was a positive correlation with the superotemporal parameter ($r = 0.277$, $p = 0.039$) ($p < 0.05$). No significant correlations were observed in any of the parameters of the other groups ($p > 0.05$).

Table 6. The correlation analysis between HbA1c and right-eye GCL++ parameters across all groups

Variables		Superior	Superonasal	Superotemporal	Inferior	Inferonasal	Inferotemporal
Control							
HbA1c	**r**	-0.152	-0.106	-0.023	-0.078	-0.017	-0.095
Prediabetes							
HbA1c	**r**	-0.138	-0.21	0.058	-0.080	-0.056	-0.093
Type I							
HbA1c	**r**	0.084	0.079	0.088	0.102	0.091	0.089
Type II							
HbA1c	**r**	0.097	0.086	0.250	0.028	0.103	0.150

[r]Pearson correlation; HbA1c: Hemoglobin A1c, GCL++: ganglion cell complex

DOI: 10.5455/medscience.2026.04.088

Table 7. The correlation analysis between HbA1c and right-eye GCL+ parameters across all groups

Variables		Superior	Superonasal	Superotemporal	Inferior	Inferonasal	Inferotemporal
Control							
HbA1c	**r**	-0.444*	-0.240	-0.272	-0.179	-0.131	-0.152
Prediabetes							
HbA1c	**r**	-0.015	-0.109	-0.148	-0.091	-0.215	-0.116
Type I							
HbA1c	**r**	0.028	0.101	0.032	0.019	0.051	0.063
Type II							
HbA1c	**r**	0.058	-0.052	0.277*	0.040	0.026	0.077

[r]Pearson correlation; HbA1c: Hemoglobin A1c, GCL+: ganglion cell layer GCIPL

Discussion

The main results of the study were that GCL++ thickness and superior macular thickness were significantly higher in the Type 1 group compared to the control and prediabetes groups. GCL+ and RNFL parameters revealed no significant difference across the study population. Upon examination of the correlation analyses, no significant correlation was found between HbA1c levels and GCL++ thickness in any group; however, in the GCL+ parameter, a negative correlation was observed in the superior region of the control group, whereas a positive correlation was identified in the superotemporal region of the Type 2 DM group. The study demonstrates that the early neurodegenerative process associated with diabetes progresses through distinct structural changes independent of current HbA1c levels and that the GCL++ complex is the most sensitive region reflecting this cellular stress.

A study in the literature has reported that IOP values in diabetic patients are significantly higher than those in a non-diabetic control group [15]. In another study comparing diabetic patients with a ruled-out diagnosis of glaucoma to healthy individuals, the authors reported that the mean IOP was significantly higher in the diabetic group [16]. Although it has been observed in the literature that IOP values increase alongside elevations in HbA1c levels, Matsuoka et al., reported that no statistically significant relationship could be established between these two parameters in their study [6]. Similarly, in another study comparing patients with preperimetric glaucoma to healthy individuals, the researchers noted that IOP and CCT parameters were similar between the groups [17]. One possible reason for the lack of a statistically significant difference in IOP and CCT values in our study may be that the patient group consisted of patients in the early stages who had not yet developed microvascular damage at the clinical level [18,19]. In contrast, HbA1c levels were found to be significantly higher in our diabetic groups compared to the control group, as expected. Possible reasons for this include the possibility that early retinal neurodegenerative changes develop not secondary to an increase in ocular pressure but as a direct consequence of metabolic stress and neurotoxicity associated with chronic hyperglycemia [20,21].

It is well established in the literature that diabetic neurodegeneration is typically characterized by progressive thinning of the RCG [3,7]. However, it has been reported that early-stage metabolic stress resulting from chronic hyperglycemia leads to the reactive activation of Müller cells and microglia prior to the onset of permanent cell loss, thereby causing subclinical swelling and an increase in volume in retinal tissues [2]. Indeed, Carpineto et al., reported a significant thinning of RNFL thickness in patients with Type 2 DM without retinopathy; although this finding appears to differ from the thickening observed in our Type 1 DM group, it may reflect the biphasic nature of diabetic neurotoxicity over time [22]. In our study, the structural thickening observed in the Type 1 DM group, which exhibited the highest HbA1c levels, was interpreted as an acute inflammatory stress response triggered by a high glycemic burden, occurring prior to the atrophic phase of neurodegeneration. These results suggest that the GCL++ parameter may serve as a sensitive in vivo biomarker for detecting the pre-atrophic stage, in which cells are still under stress, rather than the irreversible phase in which cell death has already occurred [20]. On the other hand, the fact that RNFL and GCL+ thicknesses remained similar between groups in our study demonstrates that diabetes-related neural damage progresses in a layer-specific manner. Van Dijk et al., reported that the initial neural damage induced by diabetes begins in the inner retinal layers, where metabolic activity is higher, rather than in axonal structures such as the RNFL [7]. In our device protocol, GCL+ measures only the cell bodies, whereas the GCL++ complex also includes the inner plexiform layer, where dendritic synapses are densely located. The observation of thickening in the GCL++ layer but no difference in the GCL+ and RNFL suggests that early-stage diabetic stress has not yet affected the axons in the RNFL or isolated cell bodies; rather, the damage remains localized as inflammation within the dendritic networks where synaptic connections are located [23,24]. This comprehensive anatomical response demonstrates that OCT parameters traditionally used in the diagnosis of glaucoma also possess high clinical value when used for layer-by-layer assessment in the diabetic population [25].

DOI: 10.5455/medscience.2026.04.088

When examining the other results of our study that assessed the macular and peripapillary regions, no significant difference in peripapillary RNFL thickness was observed between the groups; however, in the macular thickness analyses, only the superior parameter of the PF showed a significant thickening in favor of Type 1 DM. It is well established in the literature that diabetic neurotoxicity does not follow a homogeneous distribution in retinal topography; in particular, the superior and inferior parafoveal regions of the macula are much more sensitive to metabolic stress and fluctuations in microvascular perfusion [26]. In our study, the observation of thickening in the PF superior parameter indicates that diabetic reactive gliosis has a regional characteristic and that the damage begins in the neuroglial networks of the macular region before reaching the peripapillary area. These results further underscore the sensitivity of SS-OCT technology in detecting very early-stage structural changes in the macular region [17]. The fact that no significant association was found between HbA1c levels and GCL++ thickness in any of the groups indicates that the thickening response in retinal structure is not a linear consequence of HbA1c levels over the past 3 months. Diabetic neurodegeneration is an independent pathophysiological process, and cellular swelling may be a "cumulative" response triggered when a specific metabolic threshold is exceeded, rather than being dose-dependent [2]. On the other hand, the positive correlation between GCL+ superotemporal and HbA1c in the Type 2 DM group suggests that chronic insulin resistance in patients with Type 2 diabetes may lead to more pronounced vascular/neural stress in certain parameters [26,27]. While the negative correlation observed in the superior parameter in the control group suggests that blood glucose levels reaching physiological upper limits in a non-diabetic population may be associated with cellular aging or mild atrophy, more specific studies are needed to determine its clinical significance.

This study has some limitations. First, the retrospective and cross-sectional design of our study precludes the establishment of a causal relationship between diabetes duration and changes in ocular parameters and limits the assessment of the long-term progression of structural alterations. Additionally, due to the retrospective design and the often asymptomatic onset of the disease, precise data regarding actual disease duration and specific systemic treatments could not be reliably obtained or included in the analysis. The fact that the study population consists of individuals over the age of 18 who meet specific criteria is another factor that limits the generalizability of the findings to more heterogeneous groups of people with diabetes who have various comorbidities. Another limitation is the significant age and BMI differences among the groups. The younger age of the Type 1 DM cohort reflects the natural onset of the disease. However, since aging naturally affects retinal thickness, this demographic imbalance might be a confounding factor influencing the structural variations, necessitating future age-matched prospective studies. Another limitation is the relatively small sample size and the single-center design of the study; this limits the generalizability of the findings to broader populations. However, this seemingly limited sample size is a direct consequence of applying highly stringent inclusion and exclusion criteria (such as eliminating any scans with artifacts or SSI < 55) to isolate the pure effects of early diabetic neurodegeneration without the confounding variables of other ocular pathologies. Our current sample size may have been insufficient to detect subtle subclinical changes in other variables such as RNFL, GCL+, IOP, and CCT. Therefore, the absence of statistically significant differences for these specific parameters should be interpreted with caution, and the risk of a Type II error should be considered. Furthermore, given the large number of OCT parameters evaluated across multiple groups, we did not apply adjustments for multiple comparisons (e.g., Bonferroni correction). Consequently, the potential for Type I errors exists, and our statistically significant findings should be interpreted with appropriate caution. Also, technical factors such as eye movements or algorithmic segmentation artifacts during SS-OCT measurements may have partially affected the accuracy of the measurement results. Furthermore, the reliance on automated OCT segmentation without manual verification of the layer boundaries is a methodological limitation of this study. Given these limitations, larger-scale, multicenter, prospective studies with long-term follow-up are needed to clarify the long-term clinical outcomes of the structural adaptations we have identified.

Conclusion

The results of the study showed a significant increase in GCL++ and PF superior macular thickness in the Type 1 DM group compared to the control and prediabetes groups. The results for the RNFL, GCL+, IOP, and CCT parameters assessed by SS-OCT were found to be similar across the groups. This suggests that the classic atrophic neurodegenerative process in retinal tissues may not have begun yet, or that metabolic stress in the early stages is limited to localized reactive edema. The results suggest that early diabetes-related neural damage responds to cumulative stress rather than acute glycemic fluctuations and exhibits layer-specific progression prior to clinical microvascular damage. Large-scale, multicenter prospective studies could provide a more detailed characterization of the temporal and cellular characteristics of this structural adaptation in the process of diabetic neurotoxicity. Furthermore, the potential role of non-invasive, high-resolution imaging methods such as SS-OCT in layer-by-layer analysis could make significant contributions to early diagnosis, disease monitoring, and personalized neuroprotective treatment approaches. The number of studies in the literature evaluating structural changes preceding neuronal cell loss in complex inner retinal layers, such as the GCL++, using SS-OCT in patients with diabetes is quite limited, and the available data indicate that further research is needed to support findings in this area.

Ethical Approval
Ethics committee approval was obtained from the Samsun University Non-Interventional Clinical Research Ethics Committee (Approval No: 2023 11/4, Date: 07.06.2023).

Patient Consent
All patients provided routine clinical and surgical informed consent as a hospital procedure prior to the commencement of their treatments.

Conflict of Interest
The authors confirm the absence of any conflicts associated with this work.

Funding
The authors declare that they have received no financial support for the study.

References

1. Cho NH, Shaw JE, Karuranga S, et al. IDF Diabetes Atlas: Global estimates of diabetes prevalence for 2017 and projections for 2045. Diabetes Res Clin Pract. 2018;138:271-81.
2. Simó R, Hernández C; European Consortium for the Early Treatment of Diabetic Retinopathy (EUROCONDOR). Neurodegeneration in the diabetic eye: new insights and therapeutic perspectives. Trends Endocrinol Metab. 2014;25:23-33.
3. Sohn EH, van Dijk HW, Jiao C, et al. Retinal neurodegeneration may precede microvascular changes characteristic of diabetic retinopathy in diabetes mellitus. Proc Natl Acad Sci U S A. 2016;113:E2655-64.
4. Araszkiewicz A, Zozulinska-Ziolkiewicz D, Meller M, et al. Neurodegeneration of the retina in type 1 diabetic patients. Pol Arch Med Wewn. 2012;122:464-70.
5. Oshitari T, Fujimoto N, Hanawa K, et al. Effect of chronic hyperglycemia on intraocular pressure in patients with diabetes. Am J Ophthalmol. 2007;143:363-5. Erratum in: Am J Ophthalmol. 2007;144:339.
6. Matsuoka M, Ogata N, Matsuyama K, et al. Intraocular pressure in Japanese diabetic patients. Clin Ophthalmol. 2012;6:1005-9.
7. Van Dijk HW, Kok PH, Garvin M, et al. Selective loss of inner retinal layer thickness in type 1 diabetic patients with minimal diabetic retinopathy. Invest Ophthalmol Vis Sci. 2009;50:3404-9.
8. Cabrera DeBuc D, Somfai GM. Early detection of retinal thickness changes in diabetes using optical coherence tomography. Med Sci Monit. 2010;16:Mt15-21.
9. Kupersmith M, Garvin M, Wang JK, Kardon R. Early retinal ganglion cell layer thinning due to acute NAION and optic neuritis. Invest Ophthalmol Vis Sci. 2013;54:3233.
10. Gupta D, Chen PP. Glaucoma. Am Fam Physician. 2016;93:668-74.
11. Nakazawa T, Fukuchi T. What is glaucomatous optic neuropathy?. Jpn J Ophthalmol. 2020;64:243-9.
12. Echiverri A, Harrison WW. Evaluation of retinal structure and function in prediabetes. Diabetes Epidemiol Manag. 2023;12:100154.
13. Oliverio GW, Meduri A, De Salvo G, et al. OCT angiography features in diabetes mellitus type 1 and 2. Diagnostics. 2022;12:2942.
14. Satue M, Gavin A, Orduna E, et al. Reproducibility and reliability of retinal and optic disc measurements obtained with swept-source optical coherence tomography in a healthy population. Jpn J Ophthalmol. 2019;63:165-71.
15. Tan GS, Wong TY, Fong CW, Aung T. Diabetes, metabolic abnormalities, and glaucoma: the Singapore Malay Eye Study. Arch Ophthalmol. 2009;127:1354-61.
16. Akkaya S, Can E, Öztürk F. Comparison of optic nerve head topographic parameters in patients with primary open-angle glaucoma with and without diabetes mellitus. J Glaucoma. 2016;25:49-53.
17. Yeh SJ, Su YW, Chen MJ. Diagnostic ability of macular nerve fiber layer thickness measured by swept-source optical coherence tomography in preperimetric glaucoma. J Chin Med Assoc. 2024;87:722-7.
18. El-Agamy A, Alsubaie S. Corneal endothelium and central corneal thickness changes in type 2 diabetes mellitus. Clin Ophthalmol. 2017;11:481-6.
19. Opala A, Kołodziejski L, Grabska-Liberek I. Does well-controlled type 2 diabetes mellitus affect corneal endothelium? A comparative study. J Clin Med. 2025;14:5194.
20. Antonetti DA, Silva PS, Stitt AW. Current understanding of the molecular and cellular pathology of diabetic retinopathy. Nat Rev Endocrinol. 2021;17:195-206. Erratum in: Nat Rev Endocrinol. 2025;21:62.
21. Barber AJ, Gardner TW, Abcouwer SF. The significance of vascular and neural apoptosis to the pathology of diabetic retinopathy. Invest Ophthalmol Vis Sci. 2011;52:1156-63.
22. Carpineto P, Toto L, Aloia R, et al. Neuroretinal alterations in the early stages of diabetic retinopathy in patients with type 2 diabetes mellitus. Eye. 2016;30:673-9.
23. Gastinger MJ, Kunselman AR, Conboy EE, et al. Dendrite remodeling and other abnormalities in the retinal ganglion cells of Ins2Akita diabetic mice. Invest Ophthalmol Vis Sci. 2008;49:2635-42.
24. Catalani E, Cervia D. Diabetic retinopathy: a matter of retinal ganglion cell homeostasis. Neural Regen Res. 2020;15:1253-4.
25. Chhablani J, Sharma A, Goud A, et al. Neurodegeneration in type 2 diabetes: evidence from spectral-domain optical coherence tomography. Invest Ophthalmol Vis Sci. 2015;56:6333-8.
26. Pires I, Santos AR, Nunes S, Lobo C. Macular thickness measured by stratus optical coherence tomography in patients with diabetes type 2 and mild nonproliferative retinopathy without clinical evidence of macular edema. Ophthalmologica. 2013;229:181-6.
27. Karti O, Nalbantoglu O, Abali S, et al. Retinal ganglion cell loss in children with type 1 diabetes mellitus without diabetic retinopathy. Ophthalmic Surg Lasers Imaging Retina. 2017;48:473-7. Erratum in: Ophthalmic Surg Lasers Imaging Retina. 2017;48:530.